Experimental Investigation of Fuel Droplet Size Effects on Liquid Cloud Detonations

Taylor Brown, Rachel Hytovick, and Kareem Ahmed
University of Central Florida
Orlando, Florida, USA

1 Introduction

Liquid fuel detonations have become a critical area of investigation for the combustion community for the development of detonation-based propulsion and power generation. Detonations are significantly more thermodynamically efficient compared to deflagrations, and the high energy density of liquid fuels makes them desirable over gaseous fuels in real systems. In numerical simulations of rotating detonation combustors (RDC), liquid fuel has been shown to sustain a hydrogen-air detonation [1]. Experimentally, hydrogen addition to liquid kerosine has been shown to sustain a stable propagating detonation in an air-breathing RDC [2,3], as can pure liquid kerosine with oxygen enrichment [4].

Early work on multiphase detonations laid the groundwork with fuel sprays and fogs, proving their feasibility and present additional complexities such as atomization and breakup mechanisms [5,6]. Later work by Papavassiliou et al. captured soot foil measurements of spray detonations with various temperatures and droplet sizes, showing the cellular structure closely resembles that of gaseous detonation [7]. Recent simulations [10–12], along with early spray detonation experiments [6], suggest the size and distribution of the fuel droplets is influential to the combustion regime, detonation characteristics, and stability. Experiments by Malik et al. demonstrated detonation enhancement through RP-2 spray into an oncoming detonation [8]. This motivated an experiment that showed a purely liquid fuel detonation using a monodispersed cloud of 5μm Jet-A droplets with highly resolved diagnostics [9].

Understanding the effect of initial droplet size on detonability is necessary for design of detonation systems. The present work seeks to expand the body of experimental evidence for liquid fuel detonations using a range of small fuel droplet sizes, from 5μm to 20μm, using modern optical diagnostics to gain a better understanding of liquid fuel detonation physics.

2 Methods and Experimental Facility

For this experiment, a turbulent shock tube is used; more information regarding this facility is provided in [9]. The oxidizer used is oxygen at various levels of nitrogen dilution. The facility is filled with the

Correspondence to: kareem.ahmed@ucf.edu

Table 1: Experimental conditions with correlated theoretical properties

								Inner droplet distance (μm)					
O_2% (mass)	**N_2% (mass)**	**Φ**	**M_{CJ}**	**D_{CJ} (m/s)**	**P_{CJ} (atm)**	**$l_{ind,gas}$ (μm)**	**Mass loading ratio (α)**	**5 μm**	**8 μm**	**10 μm**	**12 μm**	**15 μm**	**20 μm**
100	0	2	9.95	2555.00	54.00	51.90	0.45	44.4	71.0	88.7	106.5	133.1	177.5
95	6	2	9.70	2523.64	52.31	58.61	0.39	46.5	74.5	93.1	111.7	139.7	186.2
89	11	2	9.44	2491.03	50.01	67.27	0.36	48.0	76.7	95.9	115.1	143.9	191.8
84	16	2	9.19	2456.67	47.53	79.31	0.31	50.5	80.9	101.1	121.3	151.6	202.1
78	22	2	8.92	2419.00	44.00	92.80	0.28	52.3	83.6	104.5	125.4	156.8	209.1
73	27	2	8.66	2381.78	42.74	109.43	0.23	55.3	88.6	110.7	132.8	166.0	221.4
68	32	2	8.39	2340.67	40.39	131.82	0.21	57.6	92.1	115.1	138.2	172.7	230.3
62	38	2	8.11	2296.57	38.20	162.65	0.17	61.3	98.2	122.7	147.2	184.0	245.4
57	43	2	7.99	2276.00	36.00	179.90	0.15	64.3	102.8	128.6	154.3	192.8	257.1
52	48	2	7.53	2197.08	34.35	268.70	0.12	69.1	110.5	138.2	165.8	207.2	276.3
47	53	2	7.41	2176.00	31.00	301.60	0.10	73.1	117.0	146.2	175.5	219.4	292.5
42	58	2	6.90	2076.57	30.42	526.81	0.08	79.5	127.3	159.1	190.9	238.6	318.2

gaseous oxidizer and then aerosolized Jet-A before ignition. The experimental diagnostics were CH* chemiluminescence and pressure measurements. The chemiluminescence was recorded at a 128x288 pixel resolution with a Photron SA-Z camera using a AF-S NIKKOR 24-85 mm f/3.5-4.5G ED VR lens. Pressure is recorded with 4 PCB Piezoelectric transducers at 500kHz-1.25MHz rates along the portion of the test section where optical diagnostics were recorded.

Table 1 provides detailed information regarding the testing conditions used. For each condition, the nitrogen and oxygen content of the oxidizer is listed, as well at the equivalence ratio, mass loading ratio, theoretical Chapman-Jouguet (CJ) pressure and velocity, and inner droplet spacing. A fuel-rich equivalence ratio of Φ=2 was used for each case. Note that Chapman-Jouguet conditions must be calculated assuming entirely vaporized fuel. The mass loading ratio is calculated using methods described by Ruiz [13].

3 Results

General Trends

In these experiments, it is shown that detonations can occur with fuel droplet sizes in the 5-15μm range. The first graph of fig. 1 shows each of the conditions tested, presented as fuel droplet size versus the oxygen percentage of the oxidizer, with the color of each point corresponding to the average V/D_{CJ} value for that condition. The average V/D_{CJ} values decrease as the nitrogen content increases across droplet size. Therefore, higher oxygen content trends to producing detonation conditions. There exists a transitional regime of conditions represented by a band of ~60% to ~15% of CJ velocity. Here, the conditions produce near-limit detonations into deflagrative combustion as the nitrogen content increases. For each droplet size, increasing nitrogen further than the most nitrogen diluted case presented in fig. 1 resulted in a non-reactive mixture, and therefore was not included.

Looking at the different droplet sizes also shows a correlation to probability of detonation. As droplet size increases, higher oxygen content is required to achieve detonation. This trend holds for the 5-15μm range of droplet sizes, where pure oxygen to ~72% oxygen and 28% nitrogen produce conditions where the average detonation velocity is close to the theoretical CJ velocity. However, for 20μm droplets, while

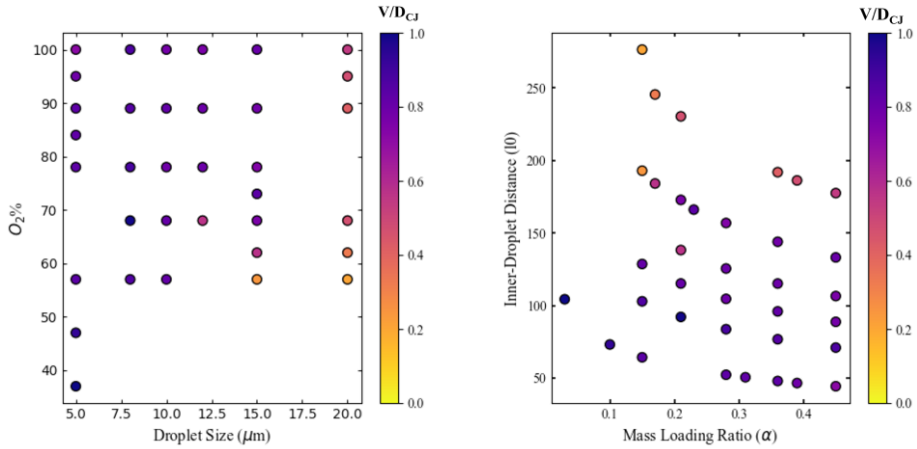

Figure 1: Droplet size vs. oxygen percentage of the oxidizer used (left) and mass loading ratio vs. inner-droplet distance (right), with a color bar corresponding to the average V/D_{CJ} value for the condition.

the chemiluminescence imaging shows a regular front typical of a detonation at the high oxygen content conditions, the associated V/D_{CJ} values are quite low, between ~0.4 and ~0.6. Notably, oxygen content still positively correlates with V/D_{CJ} for 20μm initial diameter.

The right plot shows mass loading ratio versus inter-droplet spacing. The same color bar is used as in the left side plot, scaling each condition plotted to the average V/D_{CJ} value. Higher mass loading ratios and smaller inter-droplet spacings create more favorable conditions to detonation. The biggest inner-droplet spacings, ~170μm and above, produced near-limit to deflagration conditions. These trends show that there exists an optimal range of inter-droplet spacing and mass loading ratio in which the multiphase mixture is reliably detonable. These conditions correspond to the favorable range high oxygen content and small fuel droplet size shown in the lefthand side plot.

Detonation Length Scale

Notable to liquid fuel detonations are the unique dynamics created from the persistence of droplets after the detonation front. This phenomenon has been shown both experimentally [9,14] and numerically [10,15]. Fig. 2 provides chemiluminescence imaging of detonations with fuel droplet sizes of a) 5μm, b) 10μm, c) 15μm, and d) 20μm. Each of the cases shown are with 100% O_2 and 0% N_2 for the oxidizer. High intensity at the detonation front likely correlates to this liquid fuel detonation droplet evaporation length scale. Regardless of fuel droplet size, the same phenomenon exists within the detonation as the droplets take time to undergo breakup, heating, and evaporation after the initial collision with the leading

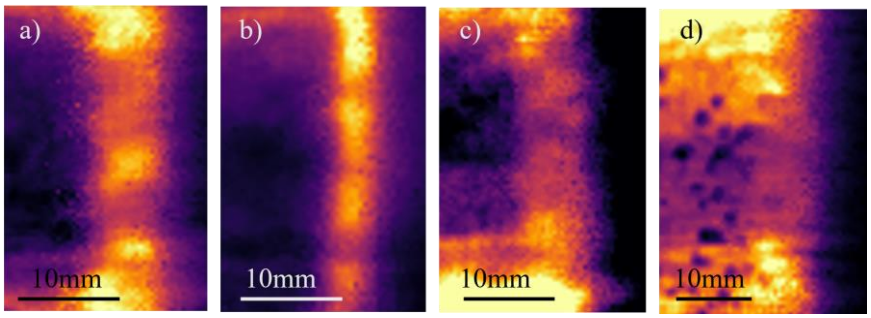

Figure 2: Chemiluminescence imaging of detonation fronts with pure oxygen at fuel droplet sizes of a) 5 micron, b) 10 micron, c) 15 micron, and d) 20 micron

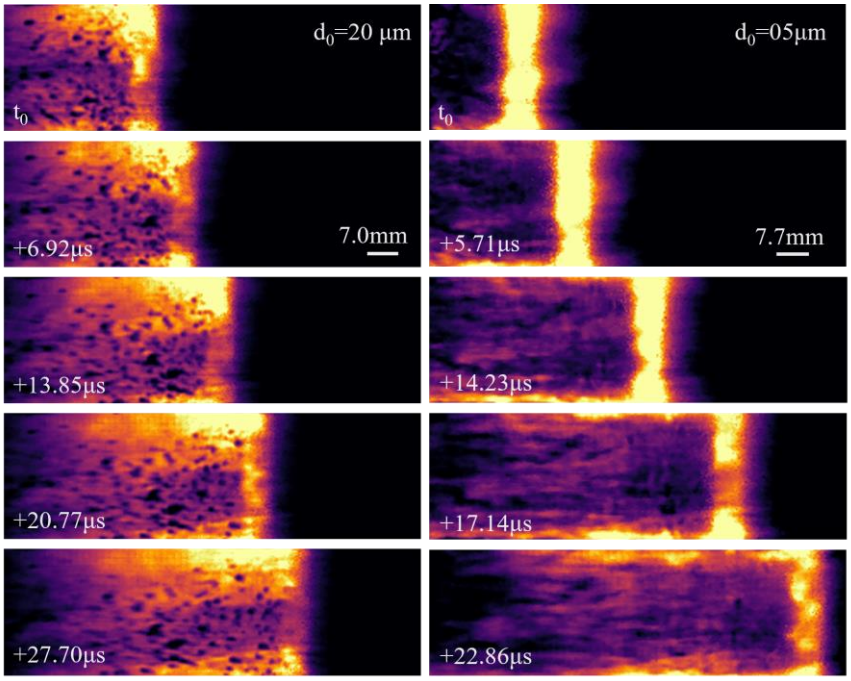

Figure 3: Chemiluminescence imaging of multiphase detonations of a) 20µm and b) 5µm fuel droplet sizes highlighting the presence of large droplets after the detonation front with 20µm droplet sizes while no droplets are visible with a 5µm droplet size

shock. Initially, the detonation front is sustained through the pre-vaporized portion of the fuel that sits in the quiescent fuel cloud. As the droplets are vaporized, they are then able to provide energy to the detonation and be consumed. The length of this process is likely to be dependent on the fuel droplet size. However, limitations of camera resolution prevent a quantitative analysis of the length scales present.

Role of Stokes Number in Large Droplet Sizes

It has been suggested that droplets larger than 10µm require additional pre-ignition vapor content to sustain a detonation in that it takes longer for these larger droplets to reduce to a vapor after contact with the detonation front [16,17]. Fig. 3 shows the reaction propagation where the fuel droplets are a) 20µm and b) 5µm. In the 20µm-sized droplet case there are large regions of fuel droplets clumping together and persisting beyond the detonation front, which does not exist with smaller fuel droplets.

Fig. 1 shows that none of the conditions with a 20µm fuel droplet cloud experience sufficiently large velocities with the magnitude traditionally considered a detonation. However, imaging still shows the regular reaction front typical of a detonation, as well as steady propagation. Chemiluminescence shows droplet heating and vaporization is still occurring. The velocity deficit seen in this work is analogous to the experiments of Bull et al. that show the velocity deficit from CJ condition increases with increasing droplet size [17]. The stokes number of the 5µm droplets in the detonation is 0.08 while it is 0.45 for the 20µm droplets. Being that 0.1 is generally considered the critical stokes number for the droplets to follow the flow path [18], it is likely that the 20µm droplets take too long to breakup or evaporate into small enough droplets so that the bulk of the fuel is consumed by the detonation.

The Deflagration-to-Detonation Transition in Liquid Fuels

The deflagration-to-detonation transition (DDT) is an important combustion regime in studying detonation initiation. Presented in Fig. 4 is chemiluminescence imaging of the evolution of DDT in a

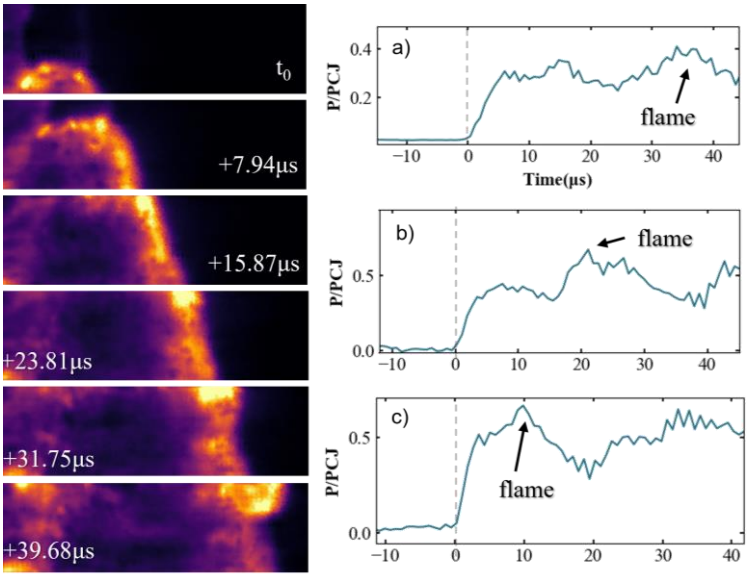

Figure 4: Chemiluminescence imaging of DDT in a liquid fuel mixture accompanied by pressure traces spaced a) 1.0 cm b) 10.5 cm, and c) 15.25 cm from where the reaction enters the optical field of view

multiphase mixture with an initial fuel droplet size of 20μm. The first image shows the initial hot-spot explosion from the wall, then the subsequent images show it propagating across the channel. In the fourth image, at +23.81μs, another hot spot forms on the opposite wall. The flame kernel expands and rapidly accelerates, sustaining the detonation transition. The pressure transducers allow for the evolution of pressure gain seen from the reaction to be recorded. From the pressure traces, the shock and flame become closer together as the transition to detonation occurs. Each of the pressure trace's times are normalized by the shock, as indicated by the dashed line at 0μs, and the proceeding shock is indicated as well.

4 Conclusion

This work presented experimental data of liquid fuel cloud detonations at small fuel droplet sizes with progressive nitrogen dilution of the oxidizer. Detonation velocities were realized for most conditions presented. Smaller fuel droplets were more conducive to detonation as nitrogen content increased, and the largest droplet size saw significant reduction in velocity compared to CJ regardless of nitrogen dilution. Generally, lower mass loading ratio and higher inner-droplet distance lends to near-limit detonations or deflagrative conditions as well. Imaging of DDT in a liquid fuel detonation was presented, with the corresponding pressure traces showing the distance between shock and flame narrowing as the DDT process evolves. Chemiluminescence imaging from across all droplet sizes show the presence of a characteristic droplet burning and evaporation length scale exists for several millimeters after the detonation front.

References

[1] M. Salvadori, A. Panchal, S. Menon, Simulation of liquid droplets combustion in a rotating detonation engine, Proceedings of the Combustion Institute 39 (2023) 3063–3072. https://doi.org/10.1016/j.proci.2022.09.002.

[2] F.A. Bykovskii, S.A. Zhdan, E.F. Vedernikov, Continuous Detonation of the Liquid Kerosene—Air Mixture with Addition of Hydrogen or Syngas, Combust Explos Shock Waves 55 (2019) 589–598. https://doi.org/10.1134/S0010508219050101.

[3] J. Kindracki, Experimental research on rotating detonation in liquid fuel-gaseous air mixtures, Aerosp Sci Technol 43 (2015) 445–453. https://doi.org/10.1016/j.ast.2015.04.006.

[4] H. Meng, Q. Zheng, C. Weng, Y. Wu, W. Feng, G. Xu, F. Wang, Propagation mode analysis of rotating detonation waves fueled by liquid kerosene, Acta Astronaut 187 (2021) 248–258. https://doi.org/10.1016/j.actaastro.2021.06.043.

[5] J.R. Bowen, K.W. Ragland, F.J. Steffes, T.G. Loflin, Heterogeneous Detonation Supported by Fuel Fogs or Films, Proceedings of the Combustion Institute Vol. 13 (1971) 1131–1139.

[6] E.K. Dabora, K.W. Ragland, J.A. Nicholls, Drop Size Effects in Spray Detonations, Proceedings of the Combustion Insitute Vol. 12 (1969) 19–26.

[7] J. Papavassiliuo, A. Makris, R. Knystautas, J.H.S. Lee, Measurements of Cellular Structure in Spray Detonation, in: Dynamic Aspects of Explosion Phenomena, American Institute of Aeronautics and Astronautics, 1993: pp. 148–169. https://doi.org/10.2514/5.9781600866272.0148.0169.

[8] V. Malik, S. Salauddin, R. Hytovick, R. Bielawski, V. Raman, J. Bennewitz, J. Burr, E. Paulson, W. Hargus, K. Ahmed, Detonation wave driven by aerosolized liquid RP-2 spray, Proceedings of the Combustion Institute 39 (2023) 2807–2815. https://doi.org/10.1016/j.proci.2022.08.127.

[9] T. Brown, R. Hytovick, J. Berson, R. Burke, S. Salauddin, K. Ahmed, Dynamics of mono-size aerosolized liquid fuel detonations, Proceedings of the Combustion Institute 40 (2024) 105416. https://doi.org/10.1016/j.proci.2024.105416.

[10] C. Tian, H. Teng, B. Shi, P. Yang, K. Wang, M. Zhao, Propagation instabilities of the oblique detonation wave in partially prevaporized n-heptane sprays, J Fluid Mech 984 (2024). https://doi.org/10.1017/jfm.2024.194.

[11] Q. Meng, S. Li, Y. Xu, H. Zhang, Droplet fragmentation effects on detonations in n-dodecane mists, Combust Flame 273 (2025). https://doi.org/10.1016/j.combustflame.2024.113944.

[12] Q. Meng, M. Zhao, Y. Xu, L. Zhang, H. Zhang, Structure and dynamics of spray detonation in n-heptane droplet/vapor/air mixtures, Combust Flame 249 (2023). https://doi.org/10.1016/j.combustflame.2022.112603.

[13] D. Martínez-Ruiz, On the structure of steady one-dimensional liquid-fueled detonations, Physics of Fluids 35 (2023). https://doi.org/10.1063/5.0162358.

[14] T. Brown, R. Hytovick, A. Morales, J. Berson, S. Salauddin, K. Chougag, K. Ahmed, Liquid fuel cloud detonation and droplet lifetime, Combust Flame 270 (2024). https://doi.org/10.1016/j.combustflame.2024.113786.

[15] D.A. Schwer, Multi-dimensional simulations of liquid-fueled jp-10/oxygen detonations, in: AIAA Propulsion and Energy Forum and Exposition, 2019, American Institute of Aeronautics and Astronautics Inc, AIAA, 2019. https://doi.org/10.2514/6.2019-4042.

[16] K. Kailasanath, Liquid-fueled detonations in tubes, J Propuls Power 22 (2006) 1261–1268. https://doi.org/10.2514/1.19624.

[17] D.C. Bull, M.A. McLeod, G.A. Mizner, Detonation of Unconfined Fuel Aerosols, in: Gasdynamics of Detonations and Explosions, American Institute of Aeronautics and Astronautics, 1981: pp. 48–60. https://doi.org/10.2514/5.9781600865497.0048.0060.